The Company of **Biologists**

RESEARCH ARTICLE

Rac1 switching at the right time and location is essential for Fcγ receptor-mediated phagosome formation

Yuka Ikeda, Katsuhisa Kawai, Akira Ikawa, Kyoko Kawamoto, Youhei Egami and Nobukazu Araki*

ABSTRACT

Lamellipodia are sheet-like cell protrusions driven by actin polymerization mainly through Rac1, a GTPase molecular switch. In Fcγ receptor-mediated phagocytosis of IgG-opsonized erythrocytes (IgG-Es), Rac1 activation is required for lamellipodial extension along the surface of IgG-Es. However, the significance of Rac1 deactivation in phagosome formation is poorly understood. Our live-cell imaging and electron microscopy revealed that RAW264 macrophages expressing a constitutively active Rac1 mutant showed defects in phagocytic cup formation, while lamellipodia were formed around IgG-Es. Because activated Rac1 reduced the phosphorylation levels of myosin light chains, failure of the cup formation is probably due to inhibition of actin/myosin II contractility. Reversible photo-manipulation of the Rac1 switch in macrophages fed with IgG-Es could phenocopy two lamellipodial motilities: outward-extension and cup-constriction by Rac1 ON and OFF, respectively. In conjunction with fluorescence resonance energy transfer imaging of Rac1 activity, we provide a novel mechanistic model of phagosome formation spatiotemporally controlled by Rac1 switching within a phagocytic cup.

KEY WORDS: Rac1, Phagocytosis, Lamellipodia, Macrophages, Live-cell imaging, Myosin, Optogenetics

INTRODUCTION

Fcγ receptor (FcγR)-mediated phagocytosis by professional phagocytes such as macrophages and neutrophils is an important host defence mechanism that mediates ingestion and destruction of immunoglobulin G (IgG)-coated pathogens. During FcγR-mediated phagocytosis, the processes of phagosome formation consisting of lamellipodial extension (phagocytic cup formation) and phagocytic cup closure (phagosome internalization) are highly dependent on actin assembly and remodelling (Aderem and Underhill, 1999; Araki et al., 1996, 2003; Swanson, 2008; Swanson et al., 1999). The actin dynamics are known to be coordinated by both phosphoinositide metabolism and Rho family GTPases by which a variety of actin-binding proteins are recruited and/or activated (Beemiller et al., 2006, 2010; Caron and Hall, 1998; Chimini and Chavrier, 2000; Csépányi-Kömi et al., 2012; Martin et al., 2016; Niedergang et al., 2016). However, the precise mechanism underlying spatiotemporal regulation of phagosome formation remains to be elucidated.

Department of Histology and Cell Biology, School of Medicine, Kagawa University, Miki, Kagawa 761-0793, Japan.

*Author for correspondence (naraki@med.kagawa-u.ac.jp)

Y.I., 0000-0003-0363-7210; N.A., 0000-0001-6160-210X

Rho family GTPases including Rac, Rho and Cdc42 function as molecular switches by cycling between two nucleotide states: GDP-bound inactive and GTP-bound active states (Ridley, 2012; Symons and Settleman, 2000). Guanine-nucleotide exchange factors (GEFs) catalyse the exchange of GDP for GTP to turn the molecular switch 'ON'. In contrast, GTPase-activation proteins (GAPs) facilitate the intrinsic GTPase activity, which catalyses GTP hydrolysis to GDP, thus turning the switch 'OFF'. These molecular switches are key regulators of actin cytoskeleton organization and are implicated in many actin-based cell functions including cell adhesion, cell migration, membrane ruffling and endocytosis. It is generally accepted that Rac1 is essential for lamellipodial extension, whereas Cdc42 and RhoA form filopodia and stress fibres, respectively (Ridley, 2001; West et al., 2000; Wheeler et al., 2006). During cell migration, Rac1 and RhoA can antagonistically regulate each other by means of crosstalk signaling (Nimnual et al., 2003). When Rac1 promotes lamellipodial extension at the front of migrating cells, RhoA retracts the rear of the cells (Lawson and Burridge, 2014; Nimnual et al., 2003; Ridley, 2001).

In FcγR-mediated phagocytosis in macrophages, Rac1 and Cdc42 are essential for lamellipodial extension surrounding IgG-opsonized targets, while RhoA is dispensable. By contrast, complement receptor-mediated phagocytosis, which can occur without lamellipodial extension, requires only RhoA (Caron and Hall, 1998; Castellano et al., 2000; Cox et al., 1997; Massol et al., 1998). Therefore, it is most likely that local Rac1 activation underneath the plasma membrane at sites of IgG-coated particle binding is indispensable for lamellipodial extension through actin polymerization. In a contradictory report (Tzircotis et al., 2011), Rac1 RNAi knockdown did not have a substantial impact on FcγR-mediated phagocytosis. In that case, some other highly homologous GTPases such as Rac2 might have compensated for Rac1 function in phagocytosis.

So far, most studies have focused on the importance of activation of Rac1, as it has been considered that only the GTP-bound active state can transduce signals. However, fluorescence resonance energy transfer (FRET) microscopy in live macrophages demonstrated that Rac1 activation is a short-term transient event in the process of FcγR-mediated phagocytosis (Hoppe and Swanson, 2004) and phagocytosis of apoptotic cells (Nakaya et al., 2008). Curiously, a recent study revealed that some GAPs, which are capable of inactivating Rac1, are crucial for the formation of phagosomes to ingest IgG-opsonized large particles (Schlam et al., 2015). These studies imply that deactivation of Rac1 following temporal activation may play an active role in phagosome formation. However, the significance of Rac1 deactivation following activation in phagosome formation has not been fully elucidated due to the technical limitations of irreversible gene silencing or overexpression. Because Rac1 behaves as a temporal switch, Rac1 ON–OFF switching at the proper time and location may be important for morphological changes in membrane

structures: from lamellipodia to phagocytic cups and intracellular phagosomes.

Therefore, in the present study, we first revealed by live-cell imaging, fluorescence and electron microscopy how a constitutively active mutant of Rac1 has an impact on the processes of phagocytosis. To further define the specific role of Rac1 ON–OFF transition, we also employed optogenetic technology using photoactivatable Rac1 (PA-Rac1), the activity of which can be reversibly manipulated by blue light illumination under a microscope (Araki et al., 2014; Wu et al., 2009).

The present study has demonstrated that Rac1 activation and deactivation at the right place and time form typical phagocytic cups that efficiently ingest IgG-opsonized particles. The deactivation of Rac1 is likely to play an active role in squeezing phagocytic cups by actin/myosin II contractile activity. Here, we provide a novel mechanistic model in which Rac1 ON–OFF switching tightly regulates phagosome formation in both space and time.

RESULTS

Expression of a constitutively active Rac1 mutant inhibits Fcγ-receptor-mediated phagocytosis

First, we examined the effect of expression of an mCitrine (a monomeric yellow fluorescent protein)-fused dominant-negative or constitutively active mutant of Rac1 on the FcγR-mediated phagocytosis of IgG-opsonized erythrocytes (IgG-Es) in RAW264 macrophages using fluorescence microscopy (Fig. 1, Fig. S1). After 8 min of IgG-E addition, actin-rich cup-shaped structures (phagocytic cups) were formed in association with IgG-Es on the dorsal surface of RAW264 cells expressing mCitrine-fused wild-type Rac1 (mCitrine–Rac1WT). However, cells expressing mCitrine–Rac1T17N, a dominant-negative mutant, showed dendrite cell morphology without actin-enriched lamellipodia or phagocytic cups on the dorsal surface. In contrast, cells expressing mCitrine–Rac1Q61L, a constitutively active mutant, had numerous actin-rich lamellipodia on the dorsal surface (Fig. S1A). After 30 min of IgG-E addition, in cells expressing mCitrine–Rac1WT,
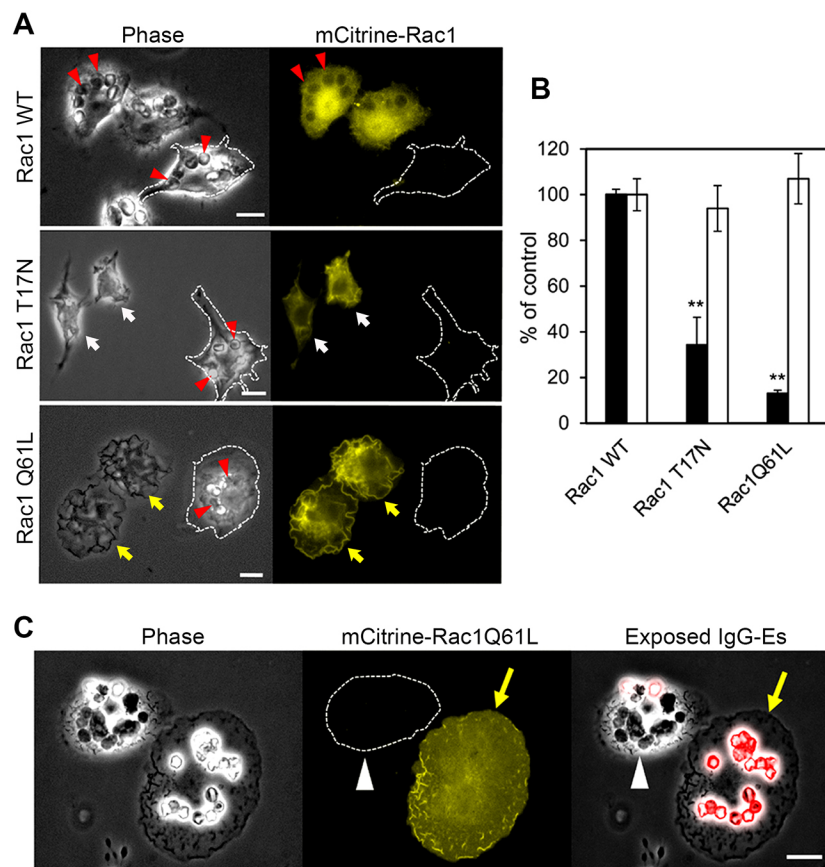

Fig. 1. Effects of overexpression of Rac1 mutants on phagocytosis of IgG-Es. (A) RAW264 cells expressing mCitrine–Rac1 wild type (WT), mCitrine–Rac1T17N GDP-locked mutant or mCitrine–Rac1Q61L GTP-locked mutant were incubated with IgG-Es for 30 min. Extracellularly exposed IgG-Es were then removed by dipping in H₂O for 30 s. The cells were fixed and observed by phase-contrast and fluorescence microscopy. Yellow fluorescent mCitrine–Rac1WT-expressing cells showed normal phagocytosis of IgG-Es (red arrowheads), similar to non-expressing cells (outlined). Cells expressing mCitrine–Rac1T17N (white arrows) did not show lamellipodium formation or phagocytosis. Cells expressing mCitrine–Rac1Q61L (yellow arrows) formed lamellipodia but failed to phagocytose IgG-Es. Scale bars: 10 μm. Images are representative of three independent experiments. (B) Quantitative analysis of the uptake (filled bars) and binding (open bars) of IgG-Es by RAW264 cells expressing Rac1WT, Rac1T17N or Rac1Q61L mutant. According to the images observed in panel A, the number of internalized IgG-Es after 30 min incubation at 37°C was scored from the 50 cells in each coverslip. The binding assay was performed by 30 min incubation with IgG-Es at 4°C followed by brief PBS wash and fixation. The results are expressed as a percentage of the control (non-expressing cells). Values represent the means±s.e.m. of four independent experiments (n=4). **P<0.01 (Student's t-test). (C) To label extracellularly exposed IgG-Es, RAW264 cells transfected with pmCitrine–Rac1Q61L were incubated with Alexa594 (red)-conjugated anti-rabbit IgG at 4°C following 30 min incubation with IgG-Es at 37°C. Even after 30 min, many IgG-Es are still left on the dorsal surface of RAW264 cells expressing mCitrine–Rac1Q61L (yellow arrows), whereas most IgG-Es were incorporated into non-expressing cells (white arrowheads). Scale bar: 10 μm.

IgG-Es were incorporated into intracellular phagosomes from which F-actin was already disassociated. However, in RAW264 cells expressing Rac1T17N or Rac1Q61L, most of the IgG-Es remain on their dorsal surface (Fig. 1C, Fig. S1B). To ensure the impact of Rac1 mutations on phagocytosis of IgG-Es, we quantified the number of IgG-Es internalized into RAW264 cells expressing mCitrine–Rac1WT, –Rac1T17N or –Rac1Q61L after 30 min incubation with IgG-Es followed by 30 s of H_2O dipping to rupture extracellularly exposed IgG-Es. Consistent with previous studies (Cox et al., 1997; Schlam et al., 2015), our quantitative assay of phagocytosis revealed that both Rac1T17N and Rac1Q61L severely inhibited uptake of IgG-Es, whereas the binding of IgG-Es to the cell surface was not significantly affected by either of them (Fig. 1B,C). These results suggest that FcγR-mediated phagocytosis of IgG-opsonized particles requires not only the GTP-bound activated state of Rac1 but also cycling between GTP-bound and GDP-bound states. Although both dominant-negative and constitutively active mutants of Rac1 inhibited phagocytosis of IgG-Es, the way of inhibiting phagocytosis may be different because there are remarkable differences in cell morphology between Rac1T17N- and Rac1Q61L-expressing cells fed with IgG-Es.

Constitutively active Rac1 produces well-developed lamellipodia but perturbs phagocytic cup formation

Lamellipodial extension requires activation of Rac1, which activates WAVE proteins and the Arp2/3 complex to stimulate actin polymerization and reorganization (Ridley, 2006; Wells et al., 2004). Therefore RAW264 cells expressing Rac1T17N fail to extend lamellipodia to engulf IgG-Es. However, it is not known why constitutively activated Rac1 hinders phagosome formation. To explore how Rac1Q61L perturbs the process of phagocytosis, we observed RAW264 cells expressing mCitrine–Rac1Q61L fed with IgG-Es by live-cell imaging. As a control, we first observed RAW264 cells expressing mCitrine–Rac1WT. Upon IgG-Es contacting with the cells, IgG-Es were promptly captured by the extending lamellipodia and engulfed in phagocytic cups. Then IgG-Es were smoothly internalized into intracellular phagosomes one by

one. It usually took less than 5 min from IgG-E binding to phagosome internalization (Fig. 2A, Movies 1 and 2).

When IgG-Es were added to cells expressing mCitrine–Rac1Q61L, lamellipodia were actively formed around IgG-Es bound on the cell surface; however, typical phagocytic cup formation was largely restrained. The lamellipodial motility in mCitrine–Rac1Q61L-expressing cells appeared to be uncoordinated for cup formation. Consequently, IgG-Es were not internalized into the cells (Fig. 2B, Movie 3).

We further observed RAW264 cells transfected with a plasmid encoding mCitrine–Rac1WT or mCitrine–Rac1Q61L by scanning electron microscopy (EM). Under scanning EM, we could not distinguish cells expressing mCitrine–Rac1WT from non-expressing cells, because their cell morphology and behaviour were almost the same. This meant that cells expressing Rac1WT phagocytosed IgG-Es in a similar way to control RAW 264 cells. When these cells were allowed to phagocytose IgG-Es for 8 min, we found that IgG-Es were captured with closely apposed lamellipodia, forming phagocytic cups (Fig. 3A, Fig. S3A). IgG-Es engulfed by the cup were deformed in cylindrical shapes, suggesting that circumferential contractile forces act on phagocytosed particles in the phagocytic cup (Araki et al., 2003). After 30 min, few IgG-Es were seen on the cell surface, because most IgG-Es had already been internalized into cells (Fig. 3B). As confirmed by the correlative light and electron microscopy (Fig. S2), RAW264 cells expressing Rac1Q61L showed the characteristic morphology of well-developed lamellipodia on their dorsal surface. Thus, we could distinguish cells expressing Rac1Q61L from non-expressing cells by the morphological features under scanning EM. After 8 min incubation with IgG-Es, long-lined lamellipodia were observed around IgG-Es bound to the dorsal surface. However, phagocytic cups closely apposed to IgG-Es were rarely seen (Fig. 3C). Even after 30 min, most IgG-Es still remained on the cell surface with lamellipodia (Fig. 3D, Fig. S3). Curiously, the morphology of lamellipodia surrounding IgG-Es was reminiscent of loose phagocytic cups observed in cells treated with ML-7, a myosin light chain kinase inhibitor (Fig. S3B,C) (Araki et al., 2003). This finding suggests that a defect in tight phagocytic cup formation in
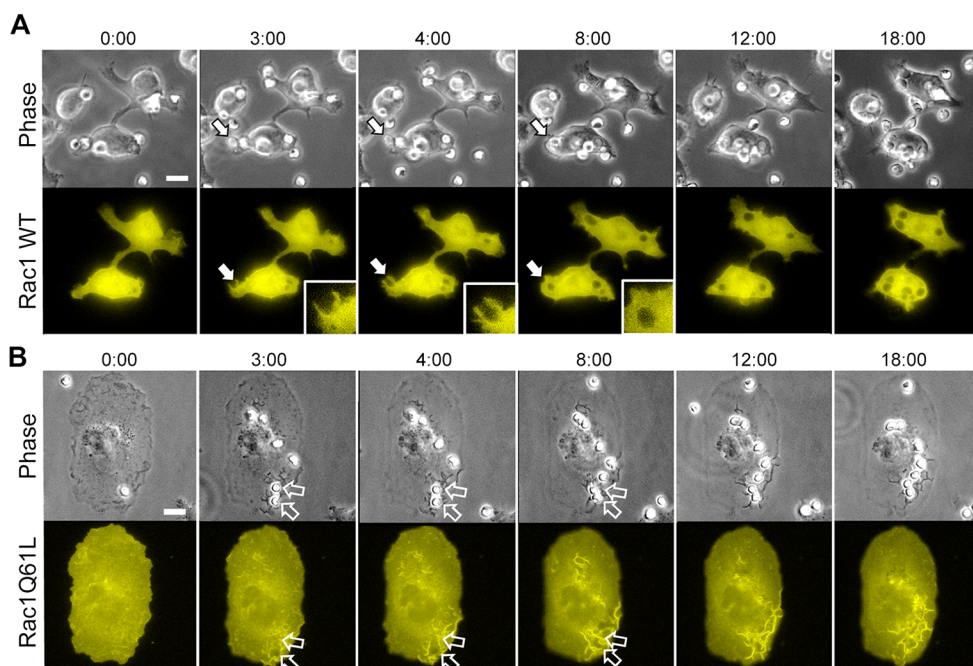

Fig. 2. Time-lapse live-cell imaging of phagocytosis by RAW264 cells expressing mCitrine–Rac1WT or constitutively active Rac1Q61L. RAW264 cells expressing mCitrine–Rac1WT (A) or mCitrine–Rac1Q61L (B) were fed with IgG-Es during time-lapse image acquisition by phase-contrast and fluorescence microscopy. (A) In mCitrine–Rac1WT-expressing cells, phagocytic cups and phagosomes were swiftly formed (arrows; magnified in inset). (B) In mCitrine–Rac1Q61L-expressing cells, no phagocytic cup or phagosome formation was observed, although active membrane ruffling was seen around IgG-Es (open arrows). Elapsed time is shown at the top (min:s). Scale bars: 10 µm.
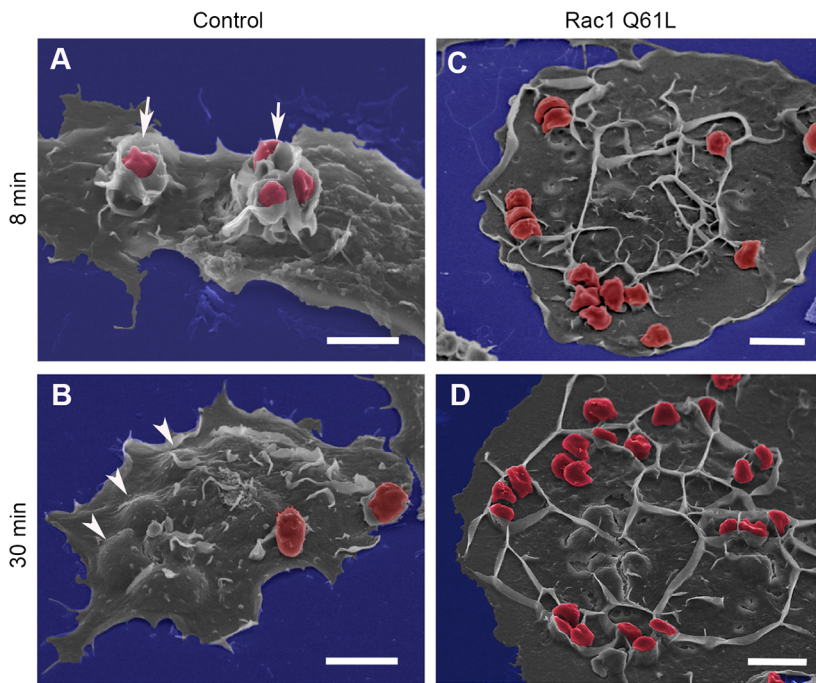
Fig. 3. Scanning electron microscopy of RAW264 cells after 8 or 30 min incubation with IgG-Es. RAW264 cells transfected with a plasmid encoding either Rac1 wild-type (Control, A,B) or constitutively active Rac1Q61L (C,D) were incubated with IgG-Es for 8 or 30 min. Cells were fixed and processed for scanning EM. Cells expressing Rac1Q61L could be identified by their characteristic morphology as shown by correlative light and electron microscopy (Fig. S2). Typical phagocytic cups engulfing IgG-Es (arrows) were observed in the control cells at 8 min (A). Arrowheads indicate IgG-Es internalized into the control cell after 30 min (B). In cells expressing Rac1Q61L, typical phagocytic cups were scarcely observed, while well-developed lamellipodia were seen (C,D). Photographs were pseudocolored by Adobe Photoshop. Scale bars: 10 µm.

Rac1Q61L-expressing cells may be due to the lack of actin/myosin-based contractile activity.

Constitutively active Rac1 suppresses phosphorylation of myosin light chains

According to the findings of live-cell imaging and scanning EM, persisting activation of Rac1 is likely to perturb lamellipodial motilities, including phagocytic cup formation. Among various downstream effectors of Rac1, p21-activated kinase 1 (PAK1) is regarded as a major effector of Rac1 in the modulation of cell motility. It was reported that PAK1 phosphorylates myosin light chain kinase (MLCK), resulting in decreased MLCK activity (Sanders et al., 1999). To examine the possibility that constitutively activated Rac1 perturbs myosin-based phagocytic cup motility by inhibiting MLCK, we observed the phosphorylated MLC (pMLC) of myosin II by immunofluorescence microscopy using an MLC phosphorylation site (Thr18/Ser19)-specific antibody. RAW264 cells expressing mCitrine–Rac1Q61L showed less immunoreaction for pMLC than non-expressing cells (Fig. S4A,B). When these cells were fed with IgG-Es or IgG-coated beads, intense pMLC immunoreactions were observed at sites of phagocytic cup formation in non-expressing cells, whereas such immunoreactions were not found in cells expressing mCitrine–Rac1Q61L (Fig. 4A–C, Fig. S4C,D). These findings indicate that constitutively activated Rac1 suppresses MLC phosphorylation, which is required for actomyosin contractility.

Localization of myosin IIB and myosin IE in a phagocytic cup

Our previous study indicated that myosin II constricts the side wall of a phagocytic cup in a PI3K-independent manner (Araki et al., 2003), whereas the cup closure is PI3K dependent (Araki et al., 1996). Myosin IE in which a tail homology 1 (TH1) domain interacts with phosphatidylinositol 3,4,5-triphosphate [PI(3,4,5)P$_3$] is known to be localized to phagocytic cups in *Dictyostelium* (Chen and Iijima, 2012; Chen et al., 2012). To characterize the role of myosin II in phagocytic cup formation in macrophages further, we compared the localizations of EGFP–myosin-IIB and mApple–myosin-IE in

phagocytic cups by live-cell imaging. Myosin IIB was first found at the bottom and side wall of the phagocytic cup. The band of myosin IIB advanced from the bottom to the top, thus squeezing the cup. However, myosin IE was more concentrated at the distal margin of the extending phagocytic cup (Fig. 4D, Movie 4). These findings are consistent with the idea that myosin II squeezes the cup from the bottom to the top, and myosin IE is involved in the extension and/or closure of the distal margin of the cup (Araki et al., 2003; Chen and Iijima, 2012; Swanson et al., 1999).

Optogenetic control of phagosome formation using photoactivatable Rac1

Because the over expression of Rac1Q61L sustained lamellipodial motility and phagocytic cup formation, it is likely that Rac1 deactivation following transient activation is crucial for the normal process of phagocytic cup formation. After outward extension of lamellipodia by Rac1 activation-driven actin polymerization, Rac1 deactivation may be required for actomyosin contractile activity to constrict the cups. To verify this hypothesis, we used the photo-manipulation system of the LOV2-domain-based photoactivatable Rac1 (PA-Rac1), which is capable of manipulating the Rac1 ON–OFF switch in live cells by illuminating with blue light (Wu et al., 2009).

When RAW264 cells expressing mCherry-fused PA-Rac1 were photoactivated with ∼430 nm light, the cells extended lamellipodia at both the cell periphery and dorsal surface. The morphology of cells was very similar to that of Rac1Q61L-expressing cells, indicating that PA-Rac1 had become switched 'ON' by the photoactivation. While PA-Rac1 was in the 'ON' state, IgG-Es bound to the cell surface did not undergo internalization to phagosomes. Within ∼10 min after turning off the illumination for PA-Rac1, some of IgG-Es were engulfed by cup-shaped lamellipodia and internalized into the cells (Fig. 5A, Movie 5). However, many IgG-Es still remained on the cell surface ∼20 min after turning off the Rac1 switch, because the rate at which IgG-Es were successfully internalized was low. Next, we alternately repeated activation and deactivation of PA-Rac1 during feeding
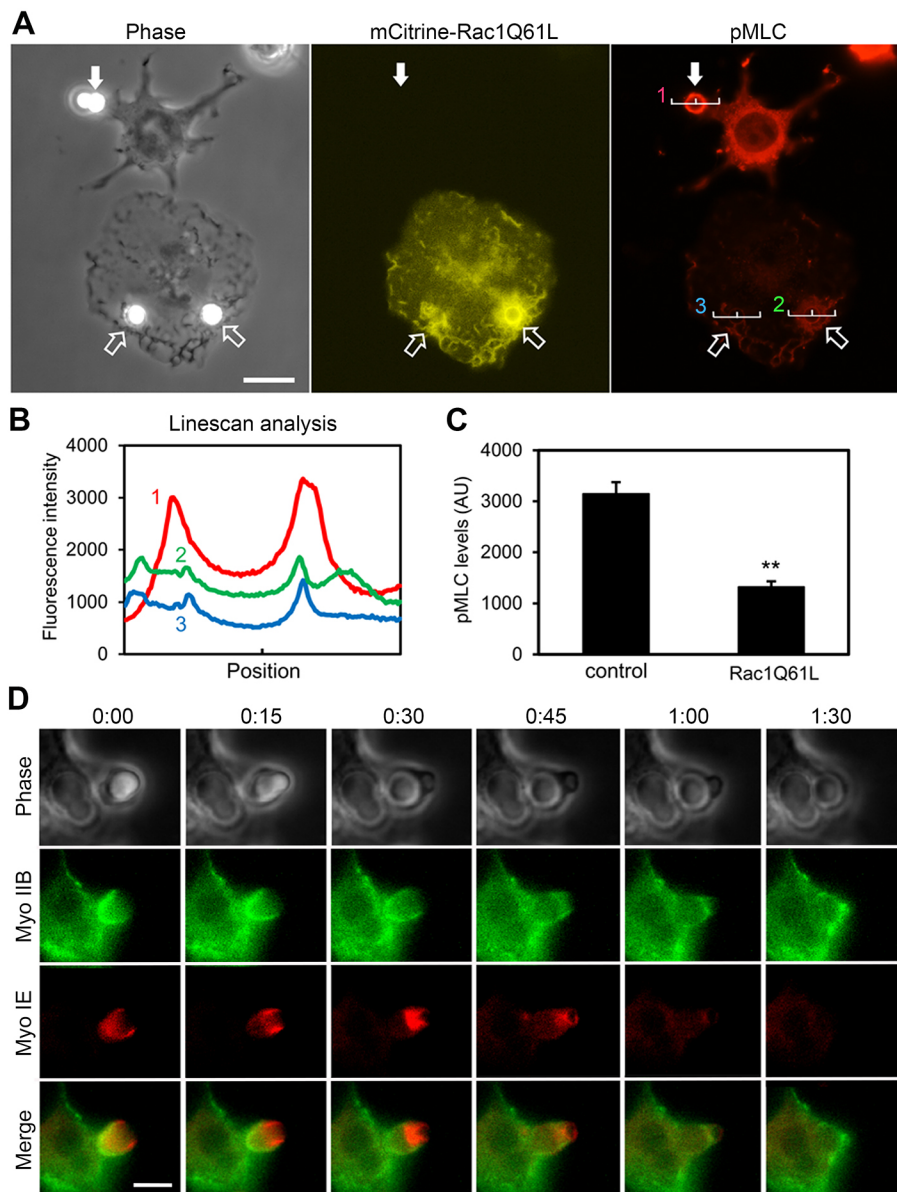
Fig. 4. Localization of myosin II and phosphorylation of myosin light chains in phagocytic cup formation.
(A) Immunofluorescence microscopy of phosphorylated myosin light chains (pMLC) in RAW264 cells expressing mCitrine–Rac1Q61L and non-expressing cells during phagocytosis of IgG-latex beads. RAW264 cells transfected with pmCitrine–Rac1Q61L were fed IgG-latex beads for 8 min, fixed and immunostained with goat anti-pMLC polyclonal antibody and Alexa594-labelled anti-goat IgG. Compared with non-expressing control cells (filled arrow), Rac1Q61L-expressing cells (open arrows) showed lower immunoreaction for pMLC, suggesting that activated Rac1 perturbs myosin II activity through inhibiting the phosphorylation of MLC. Scale bar: 10 µm. (B) Linescan analysis of the fluorescence intensity of pMLC signals at the position of lines (1, 2, 3) across phagocytic cups in the right-hand panel of A. (C) Quantitation of phosphorylation levels of MLC. Maximal values of fluorescence intensities of anti-pMLC immunoreaction at the phagocytic cup in cells expressing mCitrine–Rac1Q61L and non-expressing cells (control) were measured using MetaMorph software. Thirty phagocytic cups in each condition were assessed per replicate. Values represent the means±s.e.m. of three independent replicates (n=3). **P<0.01 (Student's t-test). (D) Time-lapse images showing dynamics of EGFP–myosin-IIB (MyoIIB, green) and mApple–myosin-IE (MyoIE, red) in a phagocytic cup engulfing IgG-E. Time elapsed from the first frame is shown as min:s. Scale bar: 5 µm.

IgG-Es. First, we photoactivated Rac1 when some IgG-Es were bound to the cell surface and then deactivated PA-Rac1 after lamellipodial extension. Also, in this case, we found that Rac1 activation caused lamellipodia to extend around IgG-Es, and its deactivation caused lamellipodia to constrict circularly and grasp IgG-Es, i.e. phagocytic cup formation. Reactivation of Rac1 caused the constricted phagocytic cups to relax. Again, the deactivation of Rac1 caused the phagocytic cup to constrict and sometimes to form intracellular phagosomes (Fig. 5B, Movie 6). The phagocytic efficiency of IgG-Es was significantly increased by repeating activation and deactivation of PA-Rac1 five times (Fig. 5C). Thus, photo-manipulation of Rac1 switching between ON and OFF states could phenocopy lamellipodial extension and constriction of the phagocytic cup.

FRET imaging demonstrates the local differential in Rac1 activity within a phagocytic cup
A previous study using FRET imaging revealed that Rac1 is transiently activated during FcγR-mediated phagocytosis (Hoppe and Swanson, 2004). However, changes in Rac1 activity within a phagocytic cup have hardly been observed probably due to limitations on the sensitivity and resolution of FRET probes. In this study, we employed a highly sensitive intramolecular FRET biosensor, Raichu–Rac1, containing an Eevee backbone (RaichuEV–Rac1) (Komatsu et al., 2011) to visualize changes in intensity and localization of Rac1 activity within a phagocytic cup. Consistent with the previous report by (Hoppe and Swanson, 2004), Rac1 activity markedly increased at sites of membrane ruffling and phagosome formation (Fig. 6A, Movies 7 and 8). A more detailed analysis of a phagocytic cup engulfing an IgG-coated 6 µm latex bead showed the local differential in Rac1 activity within the phagocytic cup. The extending portion of the cup had a higher Rac1 activity than the bottom half of the cup within ~2 min (Fig. 6B). In live-cell movies, the transient passage of Rac1 activity through a forming phagosome was more clearly demonstrated (Movies 8 and 9). These observations indicate that Rac1 is already deactivated at the portion of the cup closely apposed to IgG-opsonized particles, although it is still active in the outward-extending region of the same cup.
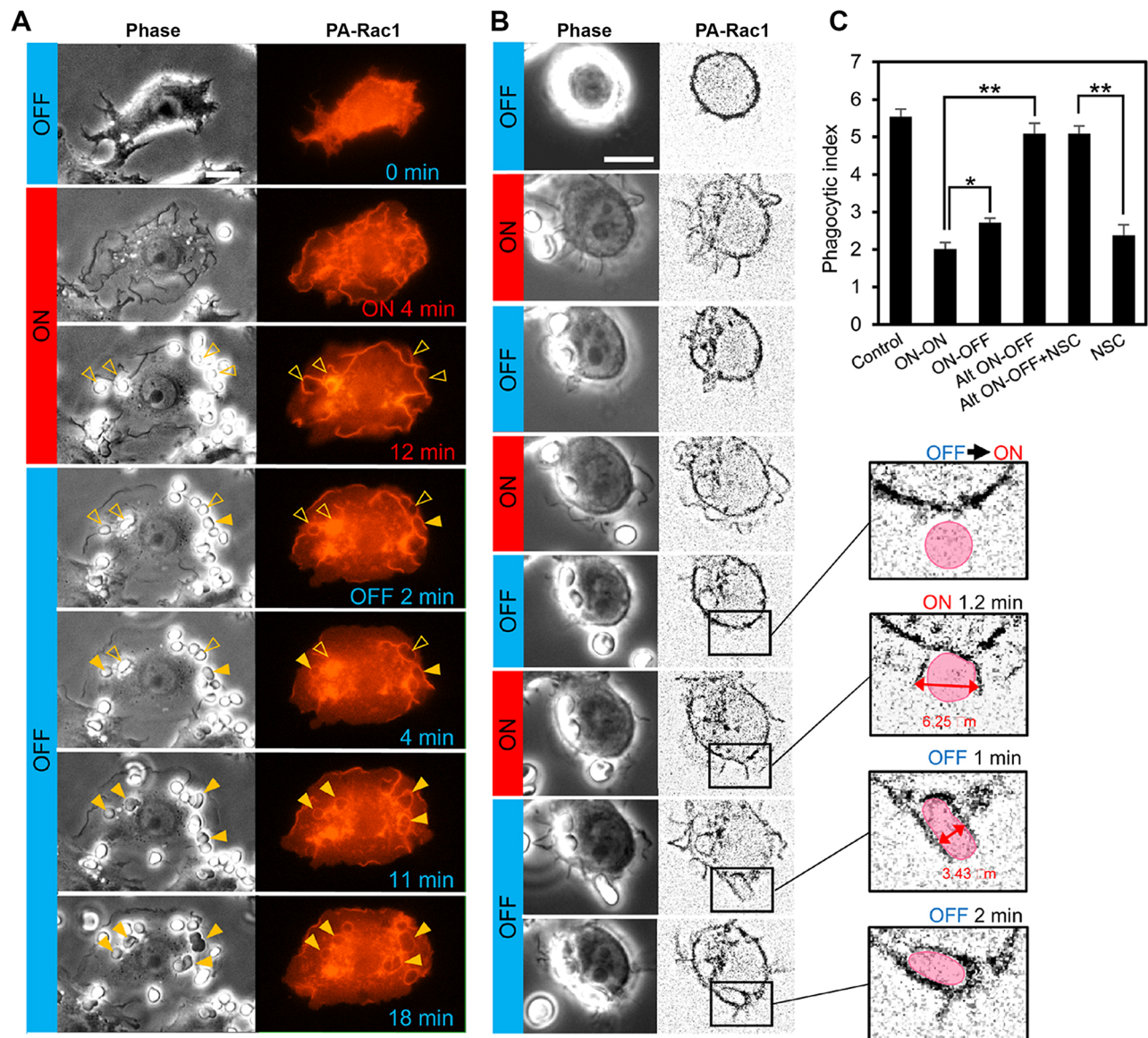
Fig. 5. Time-lapse images of optogenetic control of PA-Rac1 switch between ON and OFF in RAW264 cells fed with IgG-Es. (A) RAW264 cells expressing mCherry-fused PA-Rac1 were illuminated with ~430 nm excitation light to turn Rac1 ON during feeding on IgG-Es. Subsequently, PA-Rac1 was turned OFF by interrupting the illumination. Left: phase-contrast images. Right: mCherry–PA-Rac1 fluorescence images. Open arrowheads indicate IgG-Es bound to the cell surface. Filled arrowheads indicate phase-dark IgG-Es internalized into the cell. Scale bar: 10 μm. (B) Rac1 switching between ON and OFF was repeatedly performed during feeding with IgG-Es. Left: phase-contrast images. Right: mCherry–PA-Rac1 fluorescence images were deconvolution-processed and displayed as inverted grayscale images for perceptual contrast enhancement. The boxed areas are enlarged on the right. Scale bar: 10 μm. (C) Quantitation of phagocytic efficiency after photo-manipulation of PA-Rac1 in RAW264 cells fed with IgG-Es. Phagocytic efficiency of IgG-Es in RAW264 cells expressing mCherry-fused PA-Rac1 was assessed after 30 min phagocytosis under the following conditions of PA-Rac1 photo-manipulation: non-transfected cell (Control); ON 30 min (ON-ON); Rac1 ON and OFF 15 min each (ON-OFF); and alternate ON and OFF 3 min each five times (Alt ON-OFF). To block endogenous Rac1, 100 μM NSC 23766, a Rac1-GEF interaction inhibitor, was added (Alt ON-OFF+NSC). The effect of NSC23766 (NSC) on phagocytosis in non-expressing cells was also confirmed. After 30 min phagocytosis, extracellular IgG-Es were removed by dipping in distilled water for 30 s. After fixation, the number of internalized IgG-Es after 30 min incubation at 37°C was scored from the 30 cells in each group. The results are the means±s.e.m. of three independent experiments (*n*=3). *$P<0.05$; **$P<0.01$ (one-way ANOVA, Tukey's test).

DISCUSSION

Lamellipodia are cell membrane protrusions at the dorsal surface of adhering cells and the leading edge of migrating cells. The motility of the dorsal surface lamellipodia is often called membrane ruffling. In phagocytosis, cup-shaped lamellipodia extending along the particle surface are referred to as phagocytic cups. The formation of these lamellipodial structures is commonly dependent on actin polymerization through Rac1 activation. Locally activated Rac1 recruits WAVE2, which activates Arp2/3 complex, an actin filament nucleator. The Arp2/3 complex binds to pre-existing actin filaments and creates a branched actin filament network for extending lamellipodia during cell migration, ruffling and phagocytosis (Abou-Kheir et al., 2008; Goley and Welch, 2006; May et al., 2000; Miki et al., 2000). In this context, Rac1 activation that promotes actin polymerization through the WAVE2–Arp2/3 complex pathway could be an essential factor for lamellipodial extension at the initial step of phagocytic cup formation in macrophages.
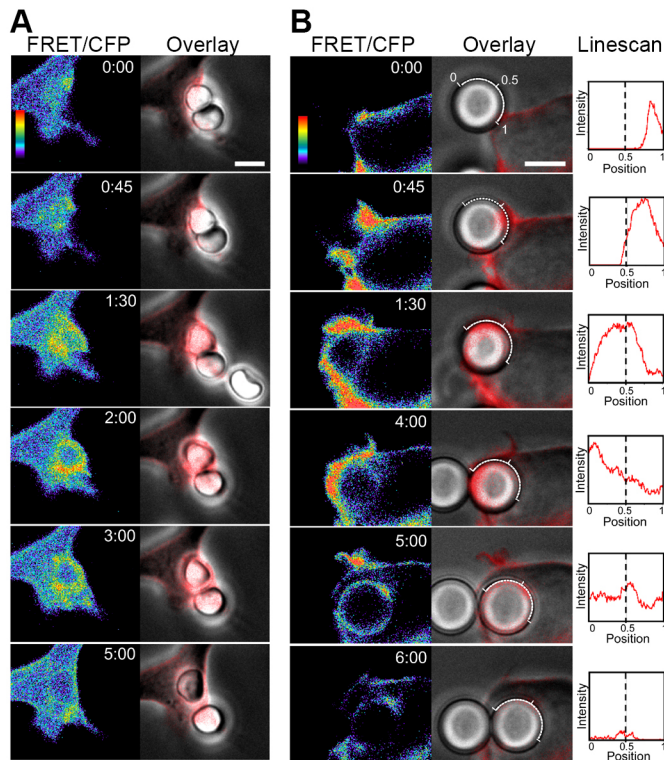
Fig. 6. FRET imaging of Rac1 activity in live RAW264 cells during phagocytosis of IgG-opsonized particles. RAW264 cells expressing RaichuEV–Rac1, a FRET biosensor for Rac1 activity, were fed with IgG-Es (A) or IgG-coated 6 µm beads (B). Ratio images showing FRET efficiency were created by the image arithmetic of the FRET/CFP ratio using MetaMorph software. Changes in FRET efficiency are shown as spectral pseudocolour (FRET/CFP). FRET efficiency images (red) were overlaid onto phase-contrast images (overlay). The FRET efficiency profile along the line in the overlay image is shown in the right panel of B at each time point. The time elapsed after the first frame is shown in each frame (min:s). The transient passage of Rac1 activity within a phagocytic cup is apparently seen in Movie 9. Scale bars: 5 µm.

In addition to the WAVE2–Arp2/3 complex pathway, GTP-bound Rac1 binds and activates PAK1. A number of proteins are known to be phosphorylated by PAK1. Among them, PAK1 phosphorylates MLCK and depresses its phosphorylation activity on myosin light chains (Sanders et al., 1999). It was reported that PAK1 localizes to membrane ruffles and phagocytic cups (Dharmawardhane et al., 1999). Furthermore, our previous study indicated that MLCK activates myosin II during FcγR-mediated phagocytosis (Araki et al., 2003), whereas the RhoA–Rho-associated protein kinase (ROCK)–myosin-II pathway is not involved in FcγR-mediated phagocytosis (Olazabal et al., 2002). Therefore it is conceivable that Rac1 activation may inhibit actomyosin contractile activity. Our immunofluorescence microscopy using a phospho-specific MLC antibody consistently demonstrated that overexpression of mCitrine–Rac1Q61L reduced the phosphorylation levels of MLC in RAW264 cells. Importantly, phosphorylated MLC (pMLC) was scarcely detected at sites of IgG-opsonized particle binding in cells overexpressing mCitrine–Rac1Q61L, whereas pMLC was abundantly localized on phagocytic cups in non-expressing cells in the same coverslip. Our scanning EM revealed that Rac1Q61L-overexpressing cells form well-developed lamellipodia around IgG-Es. However, these lamellipodia were not in close contact with IgG-Es, in contrast to the tight phagocytic cup formation

observed in non-expressing cells. Furthermore, the morphological features of loose phagocytic cups in Rac1Q61L-expressing cells were reminiscent of that observed in cells treated with an MLCK inhibitor (Fig. S2). Taken together, it is likely that constitutively activated Rac1 perturbs lamellipodial motility mainly by inhibiting actin/myosin II contractility, although some other downstream effectors of Rac1 may also directly or indirectly have an impact on phagocytic cup formation to some extent.

By live imaging of GFP-actin during phagocytosis of IgG-Es, we previously demonstrated that actin is concentrated in the extending lamellipodia that create cups (Araki et al., 2003). Subsequently, a ring-shaped actin band moves from the bottom towards the top of the cup, in such a way as to squeeze the cup and push extracellular fluid away from the phagosomes. The formation of the phagocytic cup is MLCK dependent but not PI3K dependent, although the final closure of the top aperture of the cup is PI3K dependent (Araki et al., 2003). These findings indicate that the contractile activity of the phagocytic cup side wall is driven by myosin II in a PI3K-independent manner, and that the top aperture constriction is probably driven by different classes of myosin, such as myosin I and X, which can interact with $PI(3,4,5)P_3$ (Chen et al., 2012; Cox et al., 2002; Swanson et al., 1999). In this study, we demonstrated that EGFP–myosin-IIB moves from the bottom to the top of the cup, following closely behind mApple–myosin-IE, which predominantly localizes in the extending edge. This suggests that myosin IIB constricts the side wall of the cup, whereas myosin IE may extend and/or constrict the distal edge of the cup.

Following actomyosin-ring squeezing, actin disassembly occurs at the base of the phagocytic cups. The removal of the actin coat facilitates focal exocytosis of intracellular organelles as an additional membrane source and complete phagosome internalization (Bajno et al., 2000; Schlam et al., 2015). It was also reported that PAK1 phosphorylates LIM kinase, which in turn phosphorylates cofilin and inhibits F-actin severing activity of cofilin (Edwards et al., 1999; Yang et al., 1998). Therefore, Rac1 deactivation at the bottom of the cup may also contribute to actin disassembly through the actin-severing activity of dephosphorylated cofilin. A recent report by Schlam et al. (2015) revealed that PI3K-dependent translocation of GAPs such as ARHGAP12, ARHGAP25 and SH3BP1 to phagocytic cups is responsible for the actin disassembly during the internalization of large particles. In addition, three more GAPs (GRLF1, MYO9B and PIK3R1) are recruited to phagocytic cups in a $PI(3,4,5)P_3$-independent manner (Schlam et al., 2015). Therefore, some of these $PI(3,4,5)P_3$-independent GAPs may be responsible for the Rac1 deactivation required for myosin activation.

In this study, PA-Rac1 photo-manipulation could successfully mimic lamellipodial dynamics during phagocytic cup formation in live RAW264 macrophages. After turning the Rac1 switch ON, lamellipodia vertically extended around IgG particles but did not form tight phagocytic cups. After turning the Rac1 switch OFF, the extended lamellipodia constricted to be cup-shaped and then retracted. The photo-manipulation of PA-Rac1 revealed two lamellipodial motilities, i.e. vertical extension and retraction by ON and OFF, respectively. Although circumferential constriction of phagocytic cups was also observed upon PA-Rac1 OFF, the squeezing cup movement could not be mimicked by photo-manipulation of PA-Rac1. Under normal conditions of phagosome formation, it is probable that Rac1 activation and deactivation occur at the same time in different positions within a phagocytic cup. A wave-like transition from Rac1 ON to OFF along a lamellipodium could be mediated by sequential recruitment of RhoGEFs and GAPs in parallel with $PI(4,5)P_2$ to $PI(3,4,5)P_3$

conversion by PI3K. Supporting this, we demonstrated the transitional activation of Rac1 in forming phagosomes by monitoring the Rac1 activity with a highly sensitive FRET biosensor. Rac1 was activated when IgG particles bound to the cell surface, and produced lamellipodial protrusions. Following activation, Rac1 activity decreased from the bottom of the cup (within 2 min). When Rac1 was highly active at the top part of an extending phagocytic cup, Rac1 began to be deactivated at the bottom half of the phagocytic cup (Fig. 6), suggesting that Rac1 deactivation occurred before F-actin disassembly for focal exocytosis of endomembranes at the base of the cup. The decrease of Rac1 activity shown by this FRET imaging appeared to be well correlated with cup-squeezing activity. Altogether, we can conclude that Rac1 deactivation is required for not only F-actin disassembly but also for cup contractile activity. A wave-like transition from Rac1 ON to OFF along extending lamellipodia is most likely to act as a key cause of the actin/myosin II-driven phagocytic cup squeezing. In FcγR-mediated phagocytosis of pathogenic bacteria, this squeezing activity pushing away the extra-particle fluid might decrease the phagosome volume and consequently increase the luminal concentrations of superoxide and protons needed for bacterial killing. In addition, the contraction of phagocytic cups by myosin II may promote further 'zipper-like' closure between FcγR and IgG.

Macropinocytosis is a form of non-selective fluid-phase endocytosis through the processes of membrane ruffling, circular ruffle (macropinocytic cup) formation and cup closure into macropinosomes. At both mechanistic and signaling pathway levels, macropinosome and phagosome formations share many characteristics, including their dependence on actin, PI3K and Rac1 (Swanson, 2008). Similar to the case of phagocytosis of IgG-Es, Rac1 is activated during macropinocytic cup formation and deactivated upon macropinosome closure (Yoshida et al., 2009). Nonetheless, macropinocytosis efficiently internalizes extracellular fluids into macropinosomes, while phagocytosis does not. The crucial difference between the two may be the way of deactivating Rac1 within a cup. Our previous study using the PA-Rac1 system indicated that Rac1 activation is enough to form macropinocytic cups, although deactivation is required for macropinosome closure after macropinocytic cup formation (Fujii et al., 2013). In contrast, the present study indicated that formation of typical phagocytic cups that tightly squeeze IgG-Es may require a decline of Rac1 activity before phagosome closure. It is possible that, in macropinosome formation, Rac1 in the cup wall may not be deactivated until cup closure to avoid pushing out the fluid by squeezing the cup.

On the basis of our observations, we propose a mechanistic model of FcγR-mediated phagosome formation that is spatiotemporally regulated by Rac1 switching, as follows: (1) Rac1 activation drives vertical lamellipodial extension by promoting actin polymerization; (2) Rac1 deactivation facilitates the actin/myosin II contractility of extended lamellipodia, and the close apposition of lamellipodia to the IgG-opsonized targets may assist further sequential FcγR–IgG binding in a zipper-like fashion; and (3) expansion of Rac1 deactivation from the bottom towards the top of the phagocytic cup results in cup squeezing to push fluid away from the forming phagosome (Fig. 7). To accomplish such complex tasks, Rac1 activation and deactivation need to be tightly regulated by highly ordered recruitment of RhoGEFs and GAPs to the membrane of a cup within seconds and at a submicron level. Further studies with high-resolution spatiotemporal analysis of specific GEFs and GAPs in conjunction with other signaling molecules such as phosphoinositides would be required for resolving the complexity
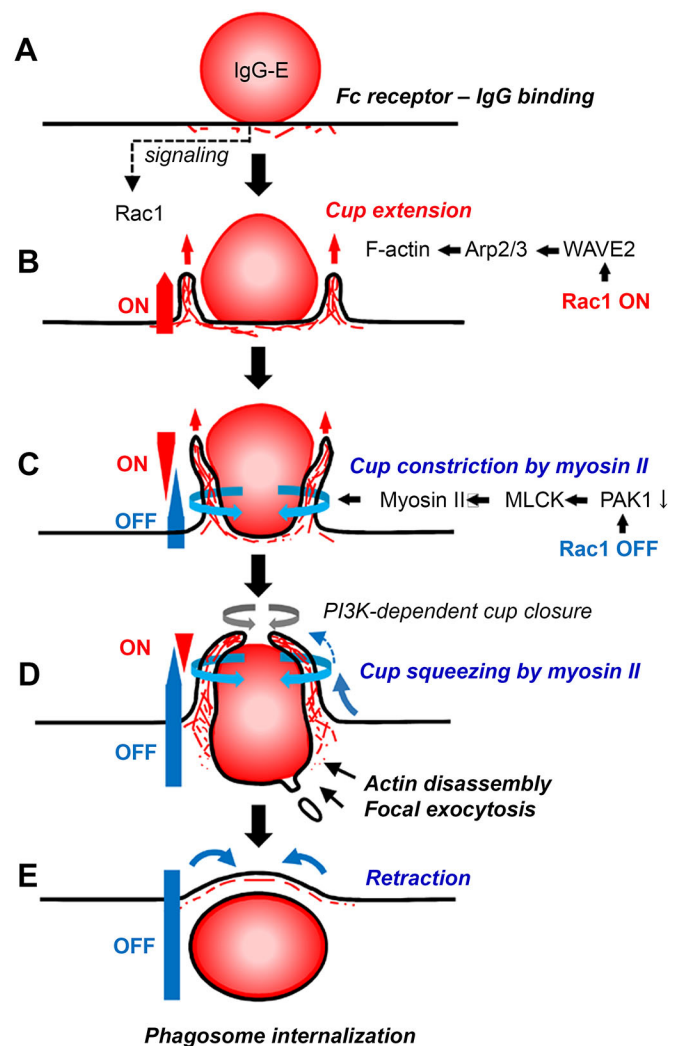

Fig. 7. Schematic model of a proposed mechanism showing phagosome formation accurately controlled by Rac1 switching in time and space. (A) IgG–Fcγ receptor binding initiates signaling to turn Rac1 ON. (B) Rac1 activation facilitates F-actin polymerization through WAVE2 and Arp2/3 (May et al., 2000). Actin polymerization produces pushing forces to make membrane protrusion around IgG-opsonized particles. (C) Deactivation of Rac1 (turn OFF) from the bottom of the cup stimulates myosin II-based contractile activity to form a tightly apposed phagocytic cup. (D) Expansion of the Rac1 OFF state region toward the cup's top squeezes the cup to push extra-particle fluid away from the forming phagosome. The final cup closure requires additional contractile activities at the tip of the cup, which may be driven by myosin IE in a PI3K-dependent manner. (E) Turning Rac1 completely OFF retracts the phagosome inside the cell and disassembles F-actin from the phagosomes to promote focal exocytosis (Schlam et al., 2015).

of the regulatory mechanism underlying Fcγ or other types of receptor-mediated phagosome formation.

MATERIALS AND METHODS
Chemicals and plasmids

FRET biosensor, Raichu–Rac1, containing an Eevee backbone (RaichuEV–Rac1) (Komatsu et al., 2011) was a gift from Dr Kazuhiro Aoki and Dr Michiyuki Matsuda (Kyoto University). Alexa594-Phalloidin was purchased from Molecular Probes (A12381). Sheep blood was obtained from Nippon Biotest Laboratory (Tokyo, Japan). Carboxylate polystyrene latex beads (6 μm in diameter, no. 17141-5) were purchased from Polysciences (Warrington, PA, USA). Other reagents were purchased from Sigma-Aldrich or Nakalai Tesque (Kyoto, Japan), unless indicated otherwise.

Cell culture and transfection

RAW264 cells were obtained from Riken Cell Bank (no. RCB0535, Tsukuba, Japan) and maintained in Dulbecco's modified Eagle's medium (DMEM) supplemented with 10% heat-inactivated fetal bovine serum (FBS) and antibiotics (100 U/ml of penicillin and 0.1 mg/ml streptomycin) at 37°C in a humidified atmosphere containing 5% CO_2. Cells were transfected with vectors for wild type or mutants of Rac1 fused with mCitrine using the Neon Transfection System (Life Technologies) according to the manufacturer's protocol. Briefly, 100 ml of a RAW264 cell suspension ($1.0{\times}10^7$ cells/ml) in Buffer R was mixed with 1.0–3.0 mg of the indicated plasmids and electroporated once at 1680 V for 20 ms. The cells were then seeded onto 13 mm or 25 mm circular coverslips in culture dishes containing DMEM. At 10–24 h after transfection, the cells were used for experiments. As a transfection control, a plasmid encoding only mCitrine was transfected to the mock cells. Cells expressing mCitrine did not show any substantial changes in phagocytosis compared with non-transfected cells.

Before the experiments, the culture medium was replaced with Ringer's buffer (RB) consisting of 155 mM NaCl, 5 mM KCl, 1 mM $MgCl_2$, 2 mM Na_2HPO_4, 10 mM glucose, 10 mM HEPES and 0.5 mg/ml bovine serum albumin (BSA) at pH 7.2

Fluorescence microscopy and quantitative analysis of FcγR phagocytosis

RAW264 cells transfected with an indicated plasmid were seeded onto 13 mm coverslips in the culture medium. Sheep erythrocytes (Es) were opsonized with rabbit anti-sheep erythrocyte IgG (no. 55806, ICN Cappel, Costa Mesa, CA, USA). For quantitative phagocytosis assay by microscopy, cells were fed with IgG-Es and incubated for 30 min in RB at 37°C. Then the coverslips were dipped in distilled water for 30 s to disrupt extracellular IgG-Es by osmotic shock. Alternatively, extracellular IgG-Es were labelled with Alexa594-conjugated anti-rabbit IgG at 4°C to distinguish extracellularly exposed (binding) IgG-Es from intracellularly incorporated (phagocytosed) ones. The cells were then fixed with 4% paraformaldehyde and 0.1% glutaraldehyde in 0.1 M phosphate buffer, pH 7.4, containing 6% sucrose for 30 min. For the IgG-Es–Fcγ receptor binding assay, cells were incubated with IgG-Es at 4°C for 15 min. After brief rinsing with cold PBS, the cells were immediately fixed without H_2O osmotic shock. Relative phagocytic/binding indexes (the phagocytic/binding efficiency of mCitrine–Rac1-expressing cells relative to non-expressing cells) of RAW264 macrophages over expressing mCitrine–Rac1 WT, constitutively active mCitrine–Rac1Q61L or dominant-negative Rac1T17N, were measured for IgG-Es by scoring the number of IgG-Es associated with 50 macrophages per coverslip. Assays for each group were performed in four independent replicates. Phagocytic/binding indexes relative to control non-expressing cells were scored from the 50 cells in each coverslip. Data are expressed as per cent of control. Values represent means±standard error of the mean (s.e.m.) of four independent experiments (n=4).

In some experiments for immunofluorescence or FRET imaging, IgG-coated latex beads were used as phagocytic targets. IgG-coated latex beads were prepared by incubation with human IgG (5 mg/ml, Sigma-Aldrich) as previously described (Chow et al., 2004).

Live-cell imaging

RAW264 cells transfected with pmCitrine-fused Rac1WT, Rac1Q61L or Rac1T17N were cultured on 25-mm circular coverslips. The coverslip was assembled in an RB-filled Attofluor cell chamber (no. A7816, Molecular Probes) and placed on a thermo-controlled stage (Tokai Hit, Shizuoka, Japan) attached to a Leica DMI 6000B inverted fluorescence microscope.

Time-lapse phase-contrast and fluorescence images of the cells were acquired at 15 s intervals through a PL Fluotar100×/1.30 NA objective lens and Orca Flash 2.8 or 4.0 CMOS camera (Hamamatsu Photonics, Hamamatsu, Japan) under the control of MetaMorph Imaging System (Molecular Devices, Sunnyvale, CA, USA).

Immunofluorescence

RAW264 cells transfected with pmCitrine–Rac1Q61L were cultured on 13-mm circular coverslips. Cells were incubated with IgG-Es or IgG-coated latex beads for 8 min in RB at 37°C and fixed with 4% paraformaldehyde in 0.1 M phosphate buffer, pH 7.4, containing 6.8% sucrose for 30 min at room temperature. After washing with PBS, cells were treated with 0.1% Triton X-100/PBS for 10 min and a blocking buffer (0.5% BSA, 0.2% gelatine, 0.1% Triton X-100 in PBS) for 20 min. Cells were then incubated with goat polyclonal anti-phosphorylated myosin light chain antibody (p-MYL9 antibody, 1:200 dilution; Santa Cruz Biotechnology) diluted with CanGet Signal B (NKB-601, Toyobo) for 90 min at room temperature. After rinsing in PBS, cells were labelled with Alexa594-labelled anti-goat IgG (1:500 dilution; Molecular Probes). Coverslips were mounted onto glass slides using a glycerol-based mounting medium and observed with an epifluorescence microscope (Leica DMI6000B) or a confocal laser microscope (Zeiss LSM700). Quantitative analysis of pMLC levels was performed by measuring fluorescence intensity of Alexa594 at the region of interest in cells using MetaMorph software.

Microscopic photo-manipulation of Rac1 switches by optogenetics

We employed a genetically encoded photoactivatable Rac1 (Wu et al., 2009) to dissect the roles of Rac1 ON and OFF in the phagocytosis of IgG-Es. RAW264 cells transfected with pTriEx/mCherry–PA-Rac1Q6L were cultured on 25-mm circular coverslips for 12–20 h. The coverslips were assembled into an RB-filled Attofluor cell chamber and placed on the 37°C thermo-controlled stage of the Leica DMI 6000B. Photoactivation of PA-Rac1 with blue light illumination was performed using a macro-program (journal menu of MetaMorph software), which automates acquisition of time-lapse images and photoactivation during the intervals of image acquisition (Araki et al., 2014). Because the light oxygen voltage 2 (LOV2) domain of PA-Rac1 is a photosensor for blue light (360–500 nm), we illuminated the cells through a cyan fluorescent protein (CFP) excitation filter (Chroma ET436/24 nm) to activate PA-Rac1. Illuminating blue light induces the conformational change of the LOV2 domain to allow downstream effector binding to Rac1, which indicates switch 'ON'. By turning off the illumination, the downstream effector binding can be reversibly hindered by the LOV2 domain (Fujii et al., 2013; Kato et al., 2014). Photo activation for live-cell imaging was performed using a 100× objective. For the quantitative assay of phagocytic efficiency combined with PA-Rac1 photo-manipulation, cells were cultured on a 13-mm circular coverslip, and photo-activated through a 4× objective to globally illuminate all cells on the coverslip. After PA-Rac1 photo-manipulation (PA-Rac1 ON for 30 min; 15 min PA-Rac1 ON for 15 min followed by OFF for 15 min; PA-Rac1 ON for 15 min followed by alternate OFF and ON 3 min each for 15 min), quantitation of phagocytic efficiency was carried out as described above. To avoid an influence of endogenous Rac1, 100 μM NSC23766, which selectively inhibits Rac1-GEF interaction but does not inhibit PA-Rac1, was added to the cells 15 min before phagocytosis of IgG-Es.

FRET imaging of Rac1 activity

To monitor the Rac1 activation state in living cells, RAW264 cells were transfected with a construct encoding RaichuEV-Rac1 (Komatsu et al., 2011), and 20–24 h after transfection, the cells were observed by the Leica DMI 6000B fluorescence microscope controlled by MetaMorph. The CFP and FRET images were acquired through ET-CFP (Chroma no. 49001) and ET-CFP/YFP FRET (Chroma no. 49052) filter sets, respectively. After background subtraction, the ratio images of the FRET/CFP, reflecting the FRET efficiency, were created with MetaMorph software as previously described (Komatsu et al., 2011). The changes in FRET efficiency were revealed as spectral pseudocolor correlated with the FRET/CFP ratio value.

Scanning electron microscopy

RAW264 cells transfected with pmCitrine–Rac1WT, pmCitrine–Rac1Q61L or pmCitrine–Rac1T17N were cultured on 4 mm by 8 mm square coverslips. The cells were allowed to phagocytose IgG-Es for the indicated times and were fixed with 4% glutaraldehyde in 0.1 M phosphate buffer, pH 7.4, for 1 h at 4°C. The specimens were post-fixed with 1% OsO_4, treated with 1% tannic acid and processed for scanning EM as previously described (Araki et al., 2003; Lu et al., 2016). The critical-point-dried cells were coated using an osmium plasma coater (OPC40, Nippon Laser & Electronics) and observed with a Hitachi S900 SEM at 6 kV. The Rac1Q61L- or Rac1T17N-expressing RAW264 macrophages could be distinguished from non-expressing cells by their morphological features (Fujii et al., 2013). In this study, we further demonstrated that RAW264 cells with a unique electron microscopic feature of well-developed long-lined ruffles are Rac1Q61L-expressing cells using correlative light and electron microscopy. After transfection with pmCitrine–Rac1Q61L, cells were cultured on coverslips printed with a grid pattern that was marked numerically in one direction and alphabetically in the other (Iwaki Glass, Shizuoka, Japan). Cells were cultured on the printed side of the coverslips. After fixation with 4% glutaraldehyde in 0.1 M phosphate buffer, pH 7.4, for 45 min, phase-contrast and fluorescence images of cells on the grid-printed coverslip were acquired by the Leica DMI 6000B microscope using a 40× objective lens. The specimens were then processed for scanning EM. The same places as observed by light microscopy were identified using the grid mark under scanning EM.

Data presentation and statistical analysis

Images are representative of ≥30 cells from at least three independent experiments. For quantitative analysis, at least 25 cells were assessed per replicate for each condition. Data presented in graphs are the means±s.e.m. of at least three independent experiments. The statistical significance of differences in mean values was determined by a two-tailed Student's t-test, or a one-way analysis of variance (ANOVA) followed by Tukey's test. P values less than 0.05 were considered statistically significant.

Author contributions

Y.I. and N.A. conceived and designed the experiments; Y.I., K. Kawai., A.I., K. Kawamoto, Y.E. and N.A. prepared materials and performed the experiments; N.A. and Y.I. wrote the manuscript; N.A. supervised the whole project.

Supplementary information

Supplementary information available online at
http://jcs.biologists.org/lookup/doi/10.1242/jcs.201749.supplemental

References

Abou-Kheir, W., Isaac, B., Yamaguchi, H. and Cox, D. (2008). Membrane targeting of WAVE2 is not sufficient for WAVE2-dependent actin polymerization: a role for IRSp53 in mediating the interaction between Rac and WAVE2. *J. Cell Sci.* **121**, 379-390.

Aderem, A. and Underhill, D. M. (1999). Mechanisms of phagocytosis in macrophages. *Annu. Rev. Immunol.* **17**, 593-623.

Araki, N., Johnson, M. T. and Swanson, J. A. (1996). A role for phosphoinositide 3-kinase in the completion of macropinocytosis and phagocytosis by macrophages. *J. Cell Biol.* **135**, 1249-1260.

Araki, N., Hatae, T., Furukawa, A. and Swanson, J. A. (2003). Phosphoinositide-3-kinase-independent contractile activities associated with Fcγ-receptor-mediated phagocytosis and macropinocytosis in macrophages. *J. Cell Sci.* **116**, 247-257.

Araki, N., Ikeda, Y., Kato, T., Kawai, K., Egami, Y., Miyake, K., Tsurumaki, N. and Yamaguchi, M. (2014). Development of an automated fluorescence microscopy system for photomanipulation of genetically encoded photoactivatable proteins (optogenetics) in live cells. *Microscopy* **63**, 255-260.

Bajno, L., Peng, X.-R., Schreiber, A. D., Moore, H.-P., Trimble, W. S. and Grinstein, S. (2000). Focal exocytosis of VAMP3-containing vesicles at sites of phagosome formation. *J. Cell Biol.* **149**, 697-706.

Beemiller, P., Hoppe, A. D. and Swanson, J. A. (2006). A phosphatidylinositol-3-kinase-dependent signal transition regulates ARF1 and ARF6 during Fcγ receptor-mediated phagocytosis. *PLoS Biol.* **4**, e162.

Beemiller, P., Zhang, Y., Mohan, S., Levinsohn, E., Gaeta, I., Hoppe, A. D. and Swanson, J. A. (2010). A Cdc42 activation cycle coordinated by PI 3-kinase during Fc receptor-mediated phagocytosis. *Mol. Biol. Cell* **21**, 470-480.

Caron, E. and Hall, A. (1998). Identification of two distinct mechanisms of phagocytosis controlled by different Rho GTPases. *Science* **282**, 1717-1721.

Castellano, F., Montcourrier, P. and Chavrier, P. (2000). Membrane recruitment of Rac1 triggers phagocytosis. *J. Cell Sci.* **113**, 2955-2961.

Chen, C.-L. and Iijima, M. (2012). Myosin I. A new PIP3 effector in chemotaxis and phagocytosis. *Commun. Integr. Biol.* **5**, 294-296.

Chen, C.-L., Wang, Y., Sesaki, H. and Iijima, M. (2012). Myosin I links PIP3 signaling to remodeling of the actin cytoskeleton in chemotaxis. *Sci. Signal.* **5**, ra10.

Chimini, G. and Chavrier, P. (2000). Function of Rho family proteins in actin dynamics during phagocytosis and engulfment. *Nat. Cell Biol.* **2**, E191-E196.

Chow, C.-W., Downey, G. P., Grinstein, S., Chow, C., Downey, G. P. and Grinstein, S. (2004). Measurements of phagocytosis and phagosomal maturation. In *Current Protocols in Cell Biology*, pp. 15.7.1-15.7.33. Hoboken, NJ, USA: John Wiley & Sons, Inc.

Cox, D., Chang, P., Zhang, Q., Reddy, P. G., Bokoch, G. M. and Greenberg, S. (1997). Requirements for both Rac1 and Cdc42 in membrane ruffling and phagocytosis in leukocytes. *J. Exp. Med.* **186**, 1487-1494.

Cox, D., Berg, J. S., Cammer, M., Chinegwundoh, J. O., Dale, B. M., Cheney, R. E. and Greenberg, S. (2002). Myosin X is a downstream effector of PI(3)K during phagocytosis. *Nat. Cell Biol.* **4**, 469-477.

Csépányi-Kömi, R., Sirokmány, G., Geiszt, M. and Ligeti, E. (2012). ARHGAP25, a novel Rac GTPase-activating protein, regulates phagocytosis in human neutrophilic granulocytes. *Blood* **119**, 573-582.

Dharmawardhane, S., Brownson, D., Lennartz, M. and Bokoch, G. M. (1999). Localization of p21-activated kinase 1 (PAK1) to pseudopodia, membrane ruffles, and phagocytic cups in activated human neutrophils. *J. Leukoc. Biol.* **66**, 521-527.

Edwards, D. C., Sanders, L. C., Bokoch, G. M. and Gill, G. N. (1999). Activation of LIM-kinase by Pak1 couples Rac/Cdc42 GTPase signalling to actin cytoskeletal dynamics. *Nat. Cell Biol.* **1**, 253-259.

Fujii, M., Kawai, K., Egami, Y. and Araki, N. (2013). Dissecting the roles of Rac1 activation and deactivation in macropinocytosis using microscopic photo-manipulation. *Sci. Rep.* **3**, 2385.

Goley, E. D. and Welch, M. D. (2006). The ARP2/3 complex: an actin nucleator comes of age. *Nat. Rev. Mol. Cell Biol.* **7**, 713-726.

Hoppe, A. D. and Swanson, J. A. (2004). Cdc42, Rac1 and Rac2 display distinct patterns of activation during phagocytosis. *Mol. Biol. Cell* **15**, 3509-3519.

Kato, T., Kawai, K., Egami, Y., Kakehi, Y. and Araki, N. (2014). Rac1-dependent lamellipodial motility in prostate cancer PC-3 cells revealed by optogenetic control of Rac1 activity. *PLoS ONE* **9**, e97749.

Komatsu, N., Aoki, K., Yamada, M., Yukinaga, H., Fujita, Y., Kamioka, Y. and Matsuda, M. (2011). Development of an optimized backbone of FRET biosensors for kinases and GTPases. *Mol. Biol. Cell* **22**, 4647-4656.

Lawson, C. D. and Burridge, K. (2014). The on-off relationship of Rho and Rac during integrin-mediated adhesion and cell migration. *Small GTPases* **5**, e27958.

Lu, Y., Cao, L., Egami, Y., Kawai, K. and Araki, N. (2016). Cofilin contributes to phagocytosis of IgG-opsonized particles but not non-opsonized particles in RAW264 macrophages. *Microscopy* **65**, 233-242.

Martin, K., Reimann, A., Fritz, R. D., Ryu, H., Jeon, N. L. and Pertz, O. (2016). Spatio-temporal co-ordination of RhoA, Rac1 and Cdc42 activation during prototypical edge protrusion and retraction dynamics. *Sci. Rep.* **6**, 21901.

Massol, P., Montcourrier, P., Guillemot, J.-C. and Chavrier, P. (1998). Fc receptor-mediated phagocytosis requires CDC42 and Rac1. *EMBO J.* **17**, 6219-6229.

May, R. C., Caron, E., Hall, A. and Machesky, L. M. (2000). Involvement of the Arp2/3 complex in phagocytosis mediated by FcγR or CR3. *Nat. Cell Biol.* **2**, 246-248.

Miki, H., Yamaguchi, H., Suetsugu, S. and Takenawa, T. (2000). IRSp53 is an essential intermediate between Rac and WAVE in the regulation of membrane ruffling. *Nature* **408**, 732-735.

Nakaya, M., Kitano, M., Matsuda, M. and Nagata, S. (2008). Spatiotemporal activation of Rac1 for engulfment of apoptotic cells. *Proc. Natl. Acad. Sci. USA* **105**, 9198-9203.

Niedergang, F., Di Bartolo, V. and Alcover, A. (2016). Comparative anatomy of phagocytic and immunological synapses. *Front. Immunol.* **7**, 18.

Nimnual, A. S., Taylor, L. J. and Bar-Sagi, D. (2003). Redox-dependent downregulation of Rho by Rac. *Nat. Cell Biol.* **5**, 236-241.

Olazabal, I. M., Caron, E., May, R. C., Schilling, K., Knecht, D. A. and Machesky, L. M. (2002). Rho-kinase and myosin-II control phagocytic cup formation during CR, but not FcγR, phagocytosis. *Curr. Biol.* **12**, 1413-1418.

Ridley, A. J. (2001). Rho family proteins: coordinating cell responses. *Trends Cell Biol.* **11**, 471-477.

Ridley, A. J. (2006). Rho GTPases and actin dynamics in membrane protrusions and vesicle trafficking. *Trends Cell Biol.* **16**, 522-529.

Ridley, A. J. (2012). Historical overview of Rho GTPases. *Methods Mol. Biol.* **827**, 3-12.

Sanders, L. C., Matsumura, F., Bokoch, G. M. and de Lanerolle, P. (1999). Inhibition of myosin light chain kinase by p21-activated kinase. *Science* **283**, 2083-2085.

Schlam, D., Bagshaw, R. D., Freeman, S. A., Collins, R. F., Pawson, T., Fairn, G. D. and Grinstein, S. (2015). Phosphoinositide 3-kinase enables phagocytosis of large particles by terminating actin assembly through Rac/Cdc42 GTPase-activating proteins. *Nat. Commun.* **6**, 8623.

Swanson, J. A. (2008). Shaping cups into phagosomes and macropinosomes. *Nat. Rev. Mol. Cell Biol.* **9**, 639-649.

Swanson, J. A., Johnson, M. T., Beningo, K., Post, P., Mooseker, M. and Araki, N. (1999). A contractile activity that closes phagosomes in macrophages. *J. Cell Sci.* **112**, 307-316.

Symons, M. and Settleman, J. (2000). Rho family GTPases: more than simple switches. *Trends Cell Biol.* **10**, 415-419.

Tzircotis, G., Braga, V. M. M. and Caron, E. (2011). RhoG is required for both FcγR- and CR3-mediated phagocytosis. *J. Cell Sci.* **124**, 2897-2902.

Wells, C. M., Walmsley, M., Ooi, S., Tybulewicz, V. and Ridley, A. J. (2004). Rac1-deficient macrophages exhibit defects in cell spreading and membrane ruffling but not migration. *J. Cell Sci.* **117**, 1259-1268.

West, M. A., Prescott, A. R., Eskelinen, E.-L., Ridley, A. J. and Watts, C. (2000). Rac is required for constitutive macropinocytosis by dendritic cells but does not control its downregulation. *Curr. Biol.* **10**, 839-848.

Wheeler, A. P., Wells, C. M., Smith, S. D., Vega, F. M., Henderson, R. B., Tybulewicz, V. L. and Ridley, A. J. (2006). Rac1 and Rac2 regulate macrophage morphology but are not essential for migration. *J. Cell Sci.* **119**, 2749-2757.

Wu, Y. I., Frey, D., Lungu, O. I., Jaehrig, A., Schlichting, I., Kuhlman, B. and Hahn, K. M. (2009). A genetically encoded photoactivatable Rac controls the motility of living cells. *Nature* **461**, 104-108.

Yang, N., Higuchi, O., Ohashi, K., Nagata, K., Wada, A., Kangawa, K., Nishida, E. and Mizuno, K. (1998). Cofilin phosphorylation by LIM-kinase 1 and its role in Rac-mediated actin reorganization. *Nature* **393**, 809-812.

Yoshida, S., Hoppe, A. D., Araki, N. and Swanson, J. A. (2009). Sequential signaling in plasma-membrane domains during macropinosome formation in macrophages. *J. Cell Sci.* **122**, 3250-3261.